Journal of Photoscience (2003), Vol. 10(3), pp. 257-261

Photoluminescence Tuning of Porous Silicon by Electrochemical Etching in Mixed Electrolytes

Ki-Hwan Lee, Ki-Seok Jeon, Seung-Koo Lee and Chang-Shik Choi[1]
Department of Chemistry, Kongju National University, Kongju 314-701, Korea
[1]Research Institute for Basic Science, Kongju National University, Kongju 314-701, Korea

We have systematically studied the evolution of the photoluminescence(PL) tuning of porous silicon(PS) by electrochemical etching in various mixed electrolytes. The electrolytes employed as an etchants were mixtures of $HF:CH_3COOH:HNO_3:C_2H_5OH$ solutions where the composition ratios (%) were varied from 10:1.98:0:88.02 to 10:1.98:8.4:79.62 under constant concentration of HF and CH_3COOH with a total volume of 100 ml. Changes in the surface morphology of the samples caused by variations in the etching process were investigated by scanning electron microscopy (SEM) and atomic force microscopy (AFM). After samples are etched in various mixed electrolytes, FTIR analyses show that there is the non-photoluminescent state and the photoluminescent state simultaneously. The PL spectra show the PL tuning in the ranging from 560 to 700 nm with the increase of HNO_3 concentration. An analysis of the subsequent PL relaxation mechanism was carried out by time-correlated single photon counting (TCSPC) method. Based on experimental results, it is assumed that a red shift of the main PL peak position is related to the HNO_3 activated formation of silicon oxygen compounds. Therefore, the use of electrolyte mixtures with composition ratios can be obtained adequate and reproducible results for PL tuning.

key words: porous silicon, photoluminescence tuning, etching solution

INTRODUCTION

The interest in porous silicon (PS) is increased considerably by the observation of room temperature visible photoluminescence (PL) [1] and electroluminescence (EL) [2,3]. It opens the possibility of the development of optoelectronics, electronics and sensor applications[4] based on PS. The micro-structural and physical characteristics of PS such as thickness, volume porosity, pore size distribution, specific surface area, PL and EL are critically dependent on various processing conditions, e.g., etching solution concentration [5-8], current density [9], etching time [10], with or without illumination [11, 12] and on properties of the silicon substrate such as doping level and crystal orientation [13]. It should be noted that systematic research of the PL spectral dependence of the preparation regimes such as a series of etching solution change has not been fulfilled so far. Therefore, these factors make it difficult to obtain adequate and reproducible data of the PS structure in relation to photo-luminescent and optical properties.

In this work, we report on a systematic study of the evolution of the photoluminescence(PL) tuning of porous silicon(PS) by electrochemical etching in various mixed electrolytes. The electrolytes employed as an etchants were mixtures of $HF:CH_3COOH:HNO_3:C_2H_5OH$ solutions where the composition ratios (%) were varied from 10:1.98:0:88.02 to 10:1.98:8.4:79.62 under constant concentration of HF and CH_3COOH with a total volume of 100 ml. Changes in the surface morphology of the samples caused by variations in the etching process were investigated by scanning electron microscopy (SEM) and atomic force microscopy (AFM). In order to investigate the possible changes that might occur at the surface of PS samples in different environments, FTIR spectra were obtained. PL spectra of all the samples were obtained using a SLM 8100 fluorescence spectrophotometer. The PL spectra show the PL tuning in the ranging from 560 to 700 nm with the increase of HNO_3 concentration. We have also performed the measurement of the decay time which shows that the HNO_3 concentration of etchants provides a very important influence of PL lifetime. The experimental results obtained are explained the relationship between PS microstructure and its anodization parameters, especially, various mixed electrolytes, through steady and dynamic state PL measurements.

MATERIALS AND METHODS

Sample preparation of PS

The PS samples were formed on p-type Si(100) wafers with a resistivity of 10-20 Ωcm by standard anodization technique. The substrates were first degreased in an ultrasonic bath of acetone for 5 min and then rinsed in deionized water. After drying with

*To whom correspondence should be addressed.
E-mail : khlee@kongju.ac.kr
Received November 24, 2003; Accepted December 11 , 2003

N_2 gas, the substrates were then simply sputtered silver paste to provide a back ohmic contact for anodization. Anodization was carried out in a solution of $HF:CH_3COOH:HNO_3:C_2H_5OH$ where the composition ratios (%) were varied from 10:1.98:0: 88.02 to 10:1.98:8.4:79.62 under constant concentration of HF and CH_3COOH with a total volume of 100 ml at a constant current density of 30 mA/cm^2 for 15 min in the dark condition. The detailed etching solutions are shown in Table 1. Immediately after anodization, the samples were taken out from the cell, rinsed in deionized water and left to dry in N_2 gas.

Measuring technique

The surface morphologies of PS samples were characte-rized by SEM, and AFM which is Scanning Probe Nanoscope IIIa in tapping mode. Silicium nitride tip size was 5 nm. The reflectance infrared spectra of PS samples were measured by FTIR spectrometer (AVATAR360, Nicolet, USA). The PL spectra of PS samples measured by spectrofluorometer (SLM8100, SIM AMINCO, USA) with a 450W Xe arc lamp light source and 4 nm bandpass excitation and emission monochromators in room temperature. Temporal profiles of the PL decays were measured by using time-correlated single photon counting (TCSPC) method. The excitation source is a self mode-rocked picosecond Ti:Sapphire laser (Coherent Co.) pumped by a $Nd:YVO_4$ laser (Edinburgh Instruments). The laser output has a~3 ps pulse width, and it can span the excitation wavelength in the range of 235-300 and 350-490 nm by using nonlinear optical crystals. The instrumental response function was measured by detection of the scattered laser pulse of ca. 1 ps with quartz crystal. The resolution FWHM is 60 ps. This method allows a time resolution of about 20 ps after deconvolution.

Table 1. Conditions for the preparation of PS samples at room temperature.

	HF (%)	HNO_3 (%)	CH_3COOH (%)	C_2H_5OH (%)
A	10	0	0	90
B	10	0	1.98	88.02
C	10	0.3	1.98	87.72
D	10	0.9	1.98	87.12
E	10	1.8	1.98	86.22
F	10	3.0	1.98	85.02
G	10	4.8	1.98	83.22
H	10	6.6	1.98	81.42
I	10	8.4	1.98	79.62

RESULTS AND DISCUSSION

Figure 1 shows the effect on the pore morphologies for an increase of HNO_3 concentration in etchants. In the case of using typical etching solution of $HF:C_2H_5OH$ without HNO_3, the pore diameters and interpore spacings are small with a highly interconnected and homogeneous pore network as shown in Figure 1(A). In the presence of HNO_3, a new porous layer is reconfirmed after removal from the previous surface layer with progress of oxidation(Figure 1(E)). However, it is not likely to be the increase the porosity with a consequent reduction in nanocrystallite sizes. The cross-section image in the bottom at Figure 1(G) shows the result for a sample etched with a higher HNO_3 concentration. In this case the height of depth increases but the pore size is only slightly increased. The result of AFM investigation of PS samples prepared in the absence and presence of HNO_3 concentration is shown in Figure 2. These images are also similar to SEM images. In contrast to A sample, G sample shows that the HNO_3 electrolyte rapidly diffuses into the bottom of the PS

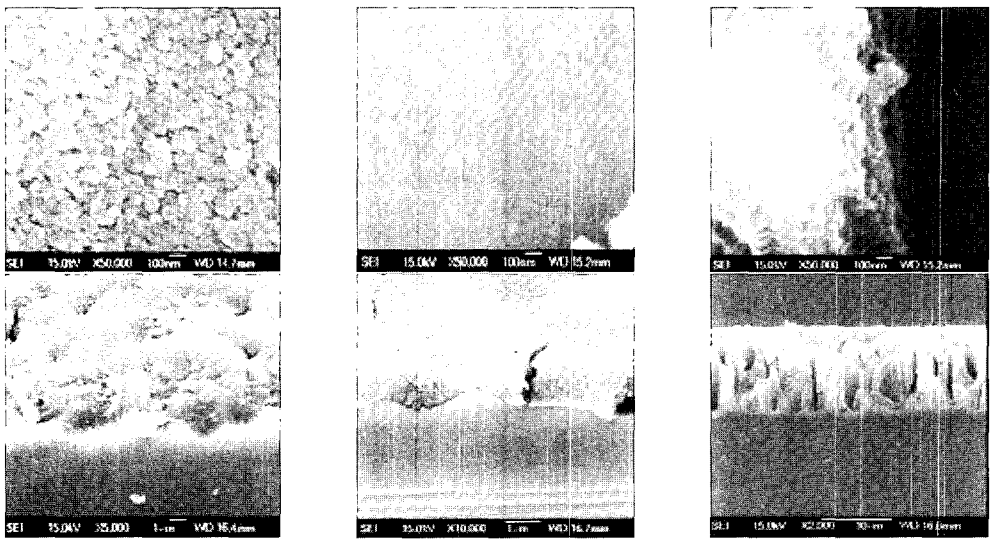

A E G

Figure 1. SEM images of PS obtained from the different electrochemical preparation conditions (for details, see table 1).

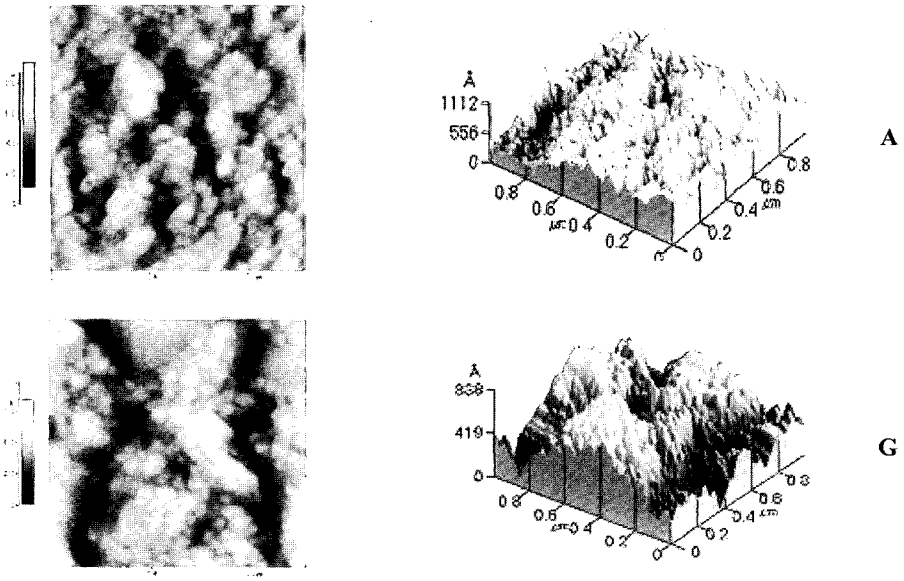

Figure 2. AFM images of PS obtained from the different electrochemical preparation conditions (for details, see table 1).

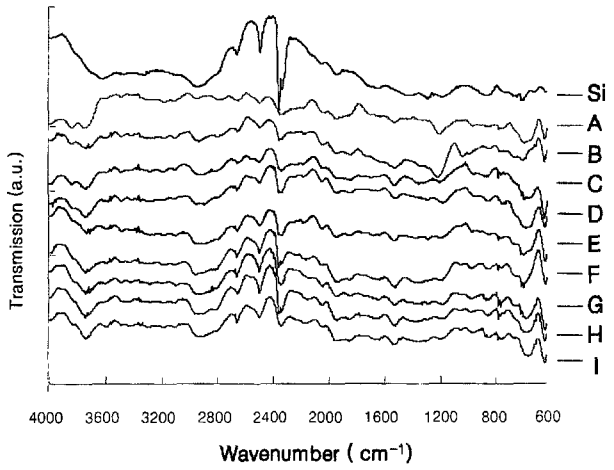

Figure 3. FTIR spectra of PS from the different electrochemical preparation conditions (for details, see table 1).

layer through the dense surface layer and the etching is formed such as a pillar structure. At the same time, the depth of the pores increases. Thus, for these samples it can be ascribed to the quantum confinement effect due to decrease of pore size.

The reflectance FTIR spectra for a PS sample prepared in the absence and presence of HNO_3 electrolyte are shown in Figure 3. From FTIR spectra, we clearly observe the presence of 2100 and 680 cm^{-1}, and 1500 cm^{-1}, which can be assigned to the Si-H and SiH_2, respectively [14-16], with the increase of HNO_3 electrolyte concentration. This indicates that the nanostructured silicon layers were reduced with the change of structure. The SEM and AFM images support this result. Thus, the retention of Si-H and SiH_2 proves that the anodization take place at the bottom of the porous layer [14]. On the other hand, the absorption peaks of around 3700, 1190 and 1100 cm^{-1} are characteristics of Si-$(OH)_x$, Si-O and Si-O-Si, respectively[17-19]. In particular, strong absorption peaks of Si-$(OH)_x$, Si-O and Si-O-Si bonds appear in the low concentration of HNO_3 electrolytes and then decreased with further increase of HNO_3 concentration. However, for the PS sample prepared in HNO_3 electrolyte concentration, these absorption peaks still remained in spite of intense Si-H and SiH_2 absorption peaks. It means that the surface layer peeled off slowly during the etching process accompanying the increase of HNO_3 concentration and then reformed the new pores below the surface. These results are expected that the PL spectra could be influenced by changing surface Si-H bonds to Si-O bonds and Si-O-Si bonds. Figure 4 shows that the evolution from the green PL, 560 nm to the red PL, 700 nm is notably enlarged with the increase of HNO_3 concentration which has not been reported before. We can see that there are resolved two types of PL-tunable range. The high energy band luminesces in the green at the photon energy band around 2.2 eV (560 nm) and the low energy band luminesces in the red around 1.8 eV (680 nm) with similar to report of Wang *et al.* [20]. In this case, the room temperature PL intensity showed an increasing trend until G sample at the presence of HNO_3 concentration and then decreased with further increase in HNO_3 concentration. Based on SEM, AFM and FTIR results, we can confirmed that both emission bands come from different ways according to the anodization conditions. Thus, the PL has the unique property that the wavelength of the emitted light can be changed by increasing or decreasing the porosity of the material in parallel with surface state. Taking into account the fact that the shifts of PL band in the presence of additional HNO_3 to lower energy in comparison with the only HF/C_2H_5OH solution (A sample),

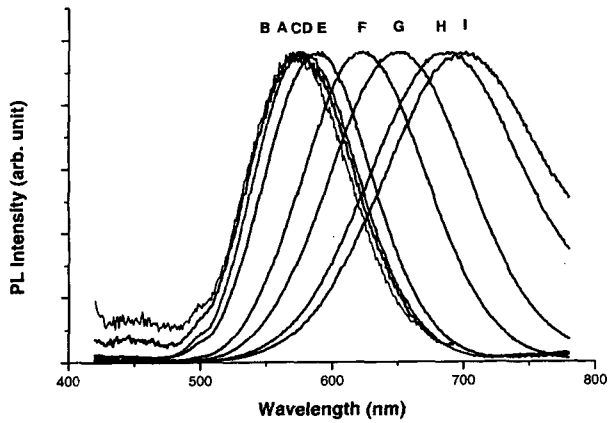

Figure 4. PL spectra of PS from the different electrochemical preparation conditions (for details, see table 1; excitation wavelength λ = 400 nm. A × 18, B × 50, C × 4.6, D × 5.8, E × 4.6, F × 2.1, G, H × 2.2, I × 2.4).

we could suppose that this band is connected with Si-H and SiH_2 groups on the Si network surface while the PL band of high energy side may be connected with Si-$(OH)_x$, Si-O and Si-O-Si groups on the Si network surface. It indicates that high energy band of PL or radiative photoluminescence centers could be connected with silicon oxide having oxidation state of the Si network while the reduction state due to Si-H and SiH_2 groups could be dominate the non-photoluminescent state. However, the steady-state data were not sufficient to provide insight into the origin of PL mechanism of PS in different mixed electrolyte condition. We used time-resolved emission spectroscopy to provide some of the required data. Considering steady-state results, it could be expected that the PL relaxation dynamics is more complicated.

The PL decay time of PS increases with increasing the HNO_3 concentration during etching condition as shown in Figure 5. That is, the high energy band has a PL decay time of about 1.11 μs(sample A), the medium energy band has a PL decay time of about 1.20 μs(sample E), and the low energy band has a decay time of 1.32 μs(sample G). The PL decay dependence studies of the high energy band and low energy band reveal distinctively different radiative electron-hole recombination mechanism. These radiative recombination from both high energy band and low energy band is a competing process. Thus, the dominant process depends on the oxidation state of the surface layer which is changed the electron-hole recombination process between the valence band and oxidative state below the conduction band [12]. The present results indicate that the appreciable increase of decay time as a function of HNO_3 concentration is consistent with that of existence of two different recombination channels. As already mentioned, therefore, the red PL shift is related to the degree of oxidation as well as quantum confinement effect.

CONCLUSION

The etching solution of electrolyte mixture having a constant composition ratios can be obtained adequate and reproducible PS.

The red shift in the presence of oxidation state can be assumed that it is governed not only the change of the electron-hole recombination mechanism between the valence band and oxidative state below the conduction band in PS but also the gradual decrease of nano-crystallite size due to the increase of oxidation state. The reason for this is considered to be attributed to the strong dependence of a slow lifetime of microsecond order. Thus, controlled oxidation by HNO_3 may lead to the desired PL spectra and its tuning.

Acknowledgment - This work was supported by a grant No. R05-2002-000-00946-0 from Korea Science & Engineering Foundation.

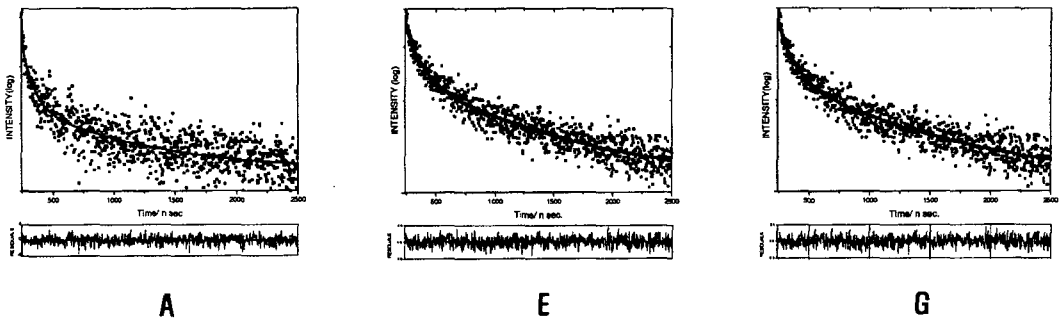

Figure 5. Measured (···) and computed (—) emission decay curves of PS samples (excitation wavelength λ = 360 nm, emission wavelength λ = 560 nm (sample A), λ = 600 nm (sample E), λ = 650 nm (sample G) ; A (τ_1=1.110 μs (87.16%), τ_2=0.109 μs (10.28%), τ_3=0.066 μs (2.56%)), E (τ_1=1.200 μs(90.74%), τ_2=0.124 μs(8.58%), τ_3=0.0627 μs (0.68%)), G (τ_1=1.320 μs (86.72%), τ_2=0.204 μs (11.63%), τ_3=0.024 μs (1.65%)).

REFERENCES

1. Canham, L. T. (1990) Silicon quantum wire array fabrication by electrochemical and chemical dissolution of wafers, *Appl.Phys. Lett.*, **57**, 1046-1048.
2. Mimura, H., Matsumoto, T. and Kanemitsu, Y. (1996) Light emitting devices using porous silicon and porous silicon carbide, *Solid-State Electronics*, **40**, 501-504.
3. Hirschman, K. D., Tsybeskev, L. Duttagupta, S. P. and Fauchet, P. M. (1996) Silicon-based visible light-emitting devices integrated into microelectronic circuits, *Nature* **384**, 338.
4. Cullis, A. G., Canham, L. T. and Calcott, P. D. J. (1997) The structural and luminescence properties of porous silicon, *J. Appl. Phys.*, **82**, 909-965.
5. Mehra, R. M., Agarwal, V. Jain, V. K. and Mathur, P. C. (1998) Influence of anodisation time, current density and electrolyte concentration on the photoconductivity spectra of porous silicon, *Thin Solid Films*. **315**, 281-285.
6. Marotti, R. E., Quagliata, E. and Dalchiele, E. A. (2003) Photoluminescence from photochemically etched silicon, *Sol. Energy Mater. Sol. Cells*, **76**, 263-279.
7. Yamamoto, N. and Takai, H. (2001) Formation mechanism of silicon based luminescence material using a photo chemical etching method, *Thin Solid Films,* **388**, 138-142.
8. Gavrilov, S. A., Belogorokhov, A. I. and Belogorokhova, L. I. (2002) A mechanism of oxygen-induced passivation of porous silicon in the HF:HCl:C_2H_5OH solutions, *Semiconductors*, **36(1)**, 98-101.
9. Korsunskaya, N. E., Torchinskaya, T. V. Dzhumaev, B. R. Khomenkova, L. Yu., and Bulakh, B. M. (1997) Two sources of excitation of photoluminescence of poroussilicon. *Semiconductors*, **31(8)**, 773-776.
10. Halimaoui, A., Oules, C. and Bomchil, G. (1991) Electroluminescence in the visible range during anodic oxidation of porous silicon films, *Appl. Phys. Lett.*, **59(3)**, 304-306.
11. Mizuno, H., Koyama, H. and Koshida, N. (1996) Oxide-free blue photoluminescence from photochemically etched porous silicon. *Appl. Phys. Lett.*, **69(25)**, 3779-3781.
12. Hossain, S. M., Chakraborty, S. Dutta, S. K. Dasand, J. and Saha, H. (2000) Stability in photoluminescence of porous silicon, *J. Lumin.*, **91**, 195-202.
13. Smith, R. L. and Collins, S. D. (1992) Porous silicon formation mechanisms, *J. Appl. Phys.*, **71**, R1-R22.
14. Shimura, Katsuma, M. M., Chikuma, T. and Okumura, T. (1999) Effect of nonaqueous anodic oxidation on the intensity of photoluminescence of porous silicon, *J. Appl. Electrochem.*, **29**, 1177-1183.
15. Ogata, Y., Niki, H. Sakka, T. and Iwasaki, M. (1995) Oxidation of Porous Silicon under Water Vapor Environment, *J. Electrochem. Soc.*, **142**, 1595-1600.
16. Ban, T., Koizumi, T. Haba, S. Koshida, N. and Suda, Y. (1994) Effects of Anodization Current Density on Photoluminescence Properties of Porous Silicon, *Jpn. J. Appl. Phys.*, **33**, 5603-5607.
17. George, M., Colvin, L. and Gupta (1988) Hydrogen desorption kinetics from monohydride and dihydride species on silicon surfaces, *Phys. Rev. B*, **37**, 8234-8243.
18. Glass, J. A. Jr, Wovchko E. A. and Yates J. T. Jr. (1995) Reaction of methanol with porous silicon, *Surf. Sci.*, **338**, 125-137.
19. Jayachandran, M., Paramasivian, M. Murali, K. R. Trivedi, D. C. and Raghaven, M. (2001) Synthesis of porous silicon nanostructures for photoluminescent devices. *Mater. Phys. Mech.*, **4**, 143-147,
20. Wang, R. Q., Li, J. J. Cai, S. M. Liu, Z. F. and Zhang, S. L. (1998) Two-peak electroluminescence of porous silicon in persulphate solution. *J. Appl. Phys.*, **72(8)**, 924- 926.